0022-3565/04/3101-311–318$20.00
THE JOURNAL OF PHARMACOLOGY AND EXPERIMENTAL THERAPEUTICS
JPET 310:311–318, 2004

Vol. 310, No. 1
63743/1152647
*Printed in U.S.A.*

# Isoproterenol Exacerbates a Long QT Phenotype in *Kcnq1*-Deficient Neonatal Mice: Possible Roles for Human-Like *Kcnq1* Isoform 1 and Slow Delayed Rectifier $K^+$ Current

Bjorn C. Knollmann,[1] Mathew C. Casimiro,[1] Alexander N. Katchman, Syevda G. Sirenko, Tilmann Schober, Qi Rong, Karl Pfeifer, and Steven N. Ebert

*Department of Pharmacology, Georgetown University Medical Center, Washington, DC (B.C.K., A.N.K., S.G.S., T.S., Q.R., S.N.E.); and Laboratory of Mammalian Genes and Development, National Institute of Child Health and Human Development/ National Institutes of Health, Bethesda, Maryland (M.C.C., K.P.)*

Received December 2, 2003; accepted February 24, 2004

## ABSTRACT

To determine whether the neonatal mouse can serve as a useful model for studying the molecular pharmacological basis of Long QT Syndrome Type 1 (LQT1), which has been linked to mutations in the human *KCNQ1* gene, we measured QT intervals from electrocardiogram (ECG) recordings of wild-type (WT) and *Kcnq1* knockout (KO) neonates before and after injection with the $\beta$-adrenergic receptor agonist, isoproterenol (0.17 mg/kg, i.p.). Modest but significant increases in JT, QT, and rate-corrected QT (QTc) intervals were found in KO neonates relative to WT siblings during baseline ECG assessments (QTc = 57 $\pm$ 3 ms, $n = 22$ versus 49 $\pm$ 2 ms, $n = 28$, respectively, $p < 0.05$). Moreover, JT, QT, and QTc intervals significantly increased following isoproterenol challenge in the KO ($p < 0.01$) but not the WT group ($p = 0.57$). Furthermore, whole-cell patch-clamp recordings show that the slow delayed rectifier $K^+$ current ($I_{Ks}$) was absent in KO but present in WT myocytes, where it was strongly enhanced by isoproterenol. This finding was confirmed by showing that the selective $I_{Ks}$ inhibitor, L-735,821, blocked $I_{Ks}$ and prolonged action potential duration in WT but not KO hearts. These data demonstrate that disruption of the Kcnq1 gene leads to loss of $I_{Ks}$, resulting in a long QT phenotype that is exacerbated by $\beta$-adrenergic stimulation. This phenotype closely reflects that observed in human LQT1 patients, suggesting that the neonatal mouse serves as a valid model for this condition. This idea is further supported by new RNA data showing that there is a high degree of homology (>88% amino acid identity) between the predominant human and mouse cardiac Kcnq1 isoforms.

Long QT Syndrome is a human disorder characterized by delayed cardiac repolarization and increased risk of developing potentially fatal ventricular arrhythmias known as "Torsades de Pointes" (Roden and Spooner, 1999). Mutations in the human *KCNQ1* (formerly *KvLQT1*) gene account for the most common form (*LQT1*) of congenital Long QT Syndrome. The *KCNQ1* gene encodes for a six-transmembrane domain voltage-gated $K^+$ channel that, when co-expressed with a $\beta$-subunit encoded by the single-transmembrane domain product of the *KCNE1* (formerly *minK*) gene, recapitulates the slow component of the cardiac-delayed rectifier $K^+$ current, $I_{Ks}$ (Barhanin et al., 1996). Consistent with the results from heterologous expression experiments, $I_{Ks}$ is absent in neonatal ventricular myocytes of *Kcne1* null mice (Drici et al., 1998). A direct link between KCNQ1 and native cardiac $I_{Ks}$ has not yet been proven, although adenoviral transfer of a G306R *KCNQ1* mutant gene has been shown to interfere with $I_{Ks}$ in isolated ventricular myocytes (Li et al., 2001).

Exercise and/or stress, which are associated with sympathetic stimulation, appear to be particularly arrhythmogenic in *LQT1* patients (Ackerman et al., 1999; Ali et al., 2000; Schwartz et al., 2001). In accordance, $I_{Ks}$ is significantly enhanced by $\beta$-adrenergic stimulation in ventricular myocytes (Walsh and Kass, 1988; An et al., 1999) via a mechanism that appears to require phosphorylation of the KCNQ1 channel by protein kinase A (PKA) (Marx et al., 2002). Thus,

This research was supported by the Pharmaceutical Research and Manufacturers of America (PhRMA) Foundation (to B.C.K.), the AHA (Grant SDG 0130285N to B.C.K.), the National Heart, Lung, and Blood Institute (Grants HL58743 to S.N.E. and HL071670 to B.C.K.), and the National Institute of Child Health and Human Development (to K.P.).

[1] These authors contributed equally to the paper.

Article, publication date, and citation information can be found at http://jpet.aspetjournals.org.
DOI: 10.1124/jpet.103.063743.

**ABBREVIATIONS:** LQT1, long QT 1 form of Long QT Syndrome; $I_{Ks}$, repolarizing $K^+$ current; PKA, protein kinase A; ECG, electrocardiogram; QTc, rate-corrected QT interval; PCR, polymerase chain reaction; RT, reverse transcription; APD, action potential duration; WT, wild type; KO, knockout; bp, base pair(s); MAP, monophasic action potential.

the absence of $I_{Ks}$ may compromise ventricular repolarization primarily during sympathetic activation.

Previously, we have shown that targeted disruption of the murine *Kcnq1* gene produces a model of Jervell and Lange-Nielson Syndrome, a disorder characterized by bilateral deafness and long QT interval (Casimiro et al., 2001). Extracardiac factors appeared to contribute to the Long QT phenotype in *Kcnq1*-deficient mice since isolated perfused $Kcnq1^{-/-}$ and $Kcnq1^{+/+}$ hearts had similar ECG profiles at baseline. We subsequently showed that sympathetic stimulation can induce a Long QT phenotype in *Kcnq1*-deficient mouse hearts since challenge with sympathethomimetic drugs such as nicotine, isoproterenol, or epinephrine produced this phenotype in the isolated perfused adult mouse heart preparation (Tosaka et al., 2003).

These data notwithstanding, characterization of cardiac phenotypes in adult $Kcnq1^{-/-}$ mice remains complicated by the fact that $Kcnq1^{-/-}$ mice have behavioral and other abnormalities due to loss of *Kcnq1* expression in the inner ear and other noncardiac tissues (Lee et al., 2000; Casimiro et al., 2001). Furthermore, it is not clear which current(s) Kcnq1 contributes to in the adult mouse heart since little or no $I_{Ks}$ have been observed in adult mouse myocytes (Wang et al., 1996; Marx et al., 2002). In contrast, fetal and neonatal mouse ventricular myocytes clearly have $I_{Ks}$ (An et al., 1996; Drici et al., 1998), and neonatal $Kcnq1^{-/-}$ mice have not yet developed the behavioral phenotypes observed in adult $Kcnq1^{-/-}$ mice. Thus, we initiated the present study to determine whether *Kcnq1* expression is necessary for $I_{Ks}$ in cardiac myocytes and to evaluate the cardiac phenotypes of neonatal $Kcnq1^{-/-}$ and $Kcnq1^{+/+}$ mice. In addition, we used RNase protection assays to more precisely characterize the 5′ end of the murine *Kcnq1* gene. These latter studies were undertaken specifically to determine whether the major mouse isoforms include the amino acid sequences demonstrated to be critical for β-adrenergic induced up-regulation of human KCNQ1 activity.

## Materials and Methods

**Drugs and Chemicals.** The rapidly activating delayed rectifier $K^+$ current-selective blocker, E-4031 (Sanguinetti and Jurkiewicz, 1990) and the $I_{Ks}$-selective blocker, L-735,821 (Selnick et al., 1997; Lengyel et al., 2001; Lynch et al., 2002) were generously provided by Eisai Co., Ltd. (Tsukuba, Japan) and Merck Research Labs (West Point, PA), respectively. All other drugs and chemicals were obtained from Sigma-Aldrich (St. Louis, MO).

**Animals.** $Kcnq1^{-/-}$ and $Kcnq1^{+/+}$ mice were generated and housed as previously described (Casimiro et al., 2001). All experiments were conducted in strict concordance with the guidelines provided by the Georgetown University Animal Care and Use Committee and the National Institutes of Health.

**Recording Electrocardiograms (ECGs) from Neonatal Mice.** ECG measurements and analyses were as described (Casimiro et al., 2001). In brief, neonatal mice (postnatal days 2–4) were anesthetized with 0.02 ml (i.p.) of 2.5% tribromoethanol solution per pup. ECGs were recorded by placing the mice in a temperature-controlled chamber immersed in a circulating water bath (37°C) and applying needle electrodes to limb regions representing leads I and II. Baseline ECGs were recorded for 3 min followed by injection with isoproterenol (0.17 mg/kg, i.p.) and an additional 5 min of continuous recording. For each lead, ECG parameters were measured from a signal-averaged (30-s record) beat using custom-built analysis software as described (Casimiro et al., 2001). The larger value from each lead was used for statistical analysis. Rate-corrected QT values (QTc) were derived using the formula QTc = QT/SQRT(RR/100) (Mitchell et al., 1998).

**Ventricular Action Potential Recordings from Isolated Neonatal Mouse Heart.** Ventricular action potentials were recorded from isolated perfused mouse hearts harvested from 3-day-old neonatal mice using a miniaturized monophasic action potential catheter as previously described for the adult mouse heart (Knollmann et al., 2001). In brief, after thoracotomy and heart removal, the aorta was cannulated using polyethylene tubing (size 10) pulled to match the size of the aorta. Retrograde perfusion was carried out at a constant perfusion pressure of 80 mm Hg at 37°C. The heart was then placed in a bath filled with the perfusion medium, where it rested horizontally in a small Perspex cradle. Krebs-Henseleit buffer containing: 118 mM NaCl, 4.7 mM KCl, 2.5 mM $CaCl_2$, 1.2 mM $MgSO_4$, 0.5 mM Na-EDTA, 25 mM $NaHCO_3$, 1.2 mM $KH_2PO_4$, and 11 mM glucose was prepared at the time of the experiment and equilibrated with a mixture of 95% $O_2$ and 5% $CO_2$ for 1 h to achieve a pH of 7.4 and a $pO_2$ of at least 500 mm Hg. Ventricular action potentials were recorded using a "miniaturized" contact electrode with a tip diameter of 0.25 mm specifically developed and validated for ventricular action potential recordings in mouse heart (Knollmann et al., 2001). MAP recordings were preamplified with a DC-coupled, isolated preamplifier with offset control (model 2000; EP Technologies, Inc., San Jose, CA). The preamplified signals were digitized at 2-kHz sampling rate and stored with the use of a commercially available data acquisition system (PowerLab; ADInstruments Pty Ltd., Castle Hill, Australia). After a stabilization period of 30 min, all hearts were perfused with Krebs-Henseleit solution containing the following: isoproterenol (200 nM) for 15 min, isoproterenol + L-735–821 (1 μM) for 15 min, and isoproterenol for 15 min. During the last 5 min of each intervention, monophasic action potentials were recorded from four to six different epicardial sites and averaged for each heart. Great care was taken to obtain measurements from corresponding sites for each intervention.

**Voltage-Clamp Recordings of Cardiac Myocytes from Neonatal Mice.** Murine ventricular myocytes were isolated on postnatal days 2 to 4, purified, and cultured as previously described (Song et al., 2002). After 2 to 3 days in culture, recordings were performed using the whole-cell patch-clamp technique (Hamill et al., 1981) with the Axopatch 200B amplifier. PCLAMP 8.0 was used for data acquisition and analysis. Time-dependent, depolarization-activated outward $K^+$ currents were recorded using a single-step protocol from a holding potential of −40 mV in response to an 8-s depolarizing step pulse to +70 mV. Tail currents were measured upon repolarization to 0 mV for 2 s. Pipettes had tip resistances of 2 to 3 MΩ when filled with solution containing: 140 mM KCI, 4 mM ATP (magnesium salt), 5 mM EGTA, 1 mM $MgCI_2$, and 10 mM HEPES, pH 7.4 (adjusted with KOH). The external solution (Tyrode's) contained: 137 mM NaCI, 5.4 mM KCI, 2 mM $CaCI_2$, 10 mM HEPES, 1 mM $MgCI_2$, and 10 mM glucose (pH 7.4, NaOH). External solution to study "slow" potassium currents (Li et al., 2001) contained: 140 mM *N*-methyl-D-glucamine, 5.4 mM KCI, 1 mM $MgCI_2$, 0.1 mM $CaCl_2$, 10 mM HEPES, 10 mM glucose (pH 7.2, HCI). Two to 5 mM 4-aminopyridine, 1 μM E 4031, 0.4 mM $CdCl_2$, or 5 μM nifedipine were added to block contaminating transient outward $K^+$ currents, rapidly activating delayed rectifier $K^+$ currents, and L-type $Ca^{2+}$ currents, respectively. All recordings were performed at room temperature (22 ± 0.5°C). Current recordings were generally stable for ≥5 min under these conditions.

**Plasmids Used to Produce Riboprobes.** MC1, MC2, and MC3 were produced by PCR from bacterial artificial chromosome clone 118L22 (Gould and Pfeifer, 1998) and cloned into the pCRII vector (Invitrogen, Carlsbad, CA) to produce the plasmids pCRII/MC1, pCRII/MC2, and pCRII/MC3. The sequences of primers used in the PCR were designed against mouse GenBank accession no. AJ251835. Primers used for MC1 (5′-GTCAGGGGTCCTGTCTGGC-3′ and 5′-CGCACTGTAGATGGAGACCC-3′) yielded a product of 305 bp.

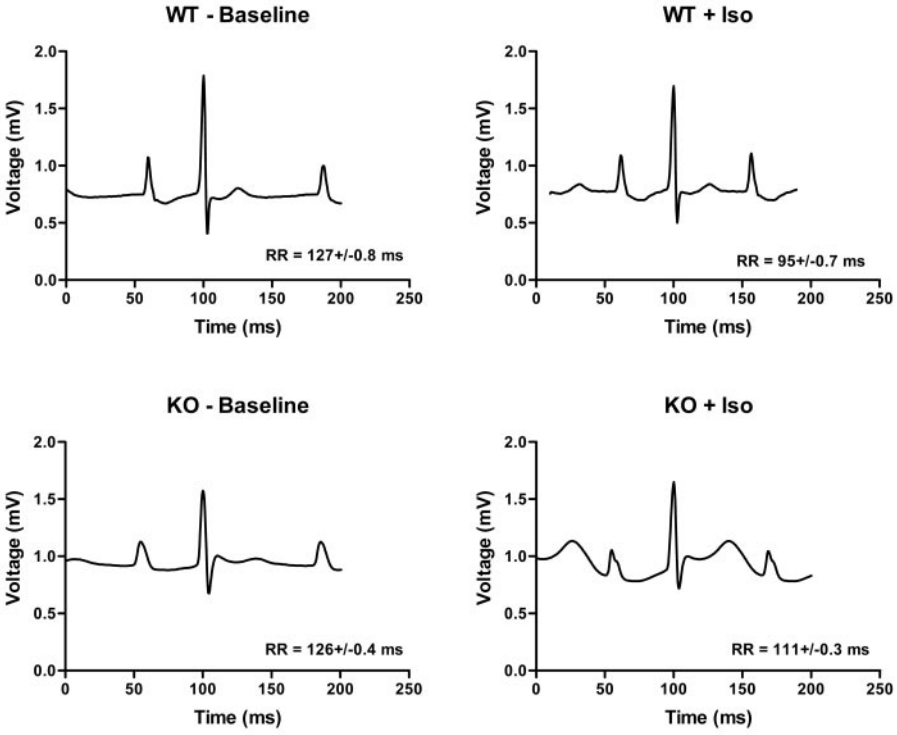


**Fig. 1.** Representative ECG recordings from anesthetized wild-type (WT) and *Kcnq1* knockout (KO) neonates before and after isoproterenol injection (0.17 mg/kg, i.p.). The ECG tracings (lead II) were signal-averaged over the 30-s period immediately preceding isoproterenol injection (Baseline) and again in the same pup approximately 3 min postinjection (Iso). Mean RR (±S.E.M.) values are indicated for each tracing shown (inset).

Primers used for MC2 (5′-GGCTTGGCGGACAGGTAACC-3′ and 5′-GGACGAGGCCGTGTCCATGG-3′) yielded a product of 269 bp. Primers used for MC3 (5′-CTGCGCCCTGCGCTCTGC-3′ and 5′-CGATGGGCGCATAGACCGTG-3′) yielded a product of 231 bp. pC1-neo/MC4 was constructed by cloning a 225-bp EcoR1-SalI fragment from pCRII/MC1 into the pC1-neo mammalian expression vector (Promega, Madison, WI) together with a 518-bp SalI-PvuI fragment from a mouse Kcnq1 cDNA clone, KP1. KP1 was cloned by reverse transcription (RT)-PCR from adult mouse heart RNA using 5′-CAGCACGGTCTATGCGCCC-3′ forward and 5′-CCCTGGACCTCCCTTGTGAG-3′ reverse primers.

**In Vitro Transcription.** The plasmids pCRII/MC1, pCRII/MC2, pCRII/MC3, and pC1-neo/MC4 were linearized with an appropriate restriction enzyme and used for in vitro runoff transcription using an RNA labeling Kit (Ambion, Austin, TX) in the presence of $^{32}$P-CTP (3000 Ci/mmol; PerkinElmer Life and Analytical Sciences, Boston, MA) to obtain the antisense riboprobes 1 to 4. The riboprobes were designed to have 5′ and 3′ nonhomologous tails derived from vector sequences adjacent to the *Kcnq1* inserts to distinguish undigested probe from protected products. The sizes of the probes (including transcribed vector sequences) were: probe 1, 390 bp; probe 2, 402 bp; probe 3, 364 bp; and probe 4, 772 bp.

**RNase Protection.** The riboprobes were gel-purified and the RNase protection assays were performed with the RPAIII kit (Ambion) according to the manufacturer's protocol. In brief, 16 $\mu$g of total RNA from mouse neonatal hearts was hybridized with the probe ($2 \times 10^5$ cpm) overnight at 58°C and 65°C and then digested with RNase A (250 U/ml) and RNAaseT1 (10,000 U/ml). Protected fragments were separated in a 0.5-mm-thick 8 M urea and 5% acrylamide gel and revealed using X-OMAT film (Eastman Kodak, Rochester, NY) exposed overnight at −80°C with an intensifying screen. The sizes of the protected products were assessed by comparison with a 100-bp RNA ladder produced from the RNA Century Marker Template Set (Ambion). Data were quantified by densitometric scanning of the film ($n = 5$) using the National Institutes of Health Image software package (http://rsb.info.nih.gov/nih-image/).

**RT-PCR.** Neonatal mouse heart RNA was used as a template to produce single-stranded cDNA using the Thermoscript RT-PCR System (Invitrogen). A 758-bp product was amplified using *Kcnq1* specific primers (5′-GTCAGGGGTCCTGTCTGGC-3′ forward and 5′-GGTACCCCCCTGGCGATCG-3′ reverse) with 30 cycles of amplification (45 s at 94°C, 45 s at 58°C, and 1 min at 72°C). The product was TOPO Cloned (Invitrogen), and both strands were sequenced (GenBank accession no. AY331142).

**Data Analysis.** All data are presented as mean ± S.E.M. Statistical significance was evaluated using the Student's $t$ test for comparison of ECG and action potential duration (APD) results, one-way analysis of variance for comparison of voltage-clamp data, and $\chi^2$ analysis for comparison of $I_{Ks}$ incidence in the absence versus the presence of Kcnq1. For all tests, $p < 0.05$ was required to reject the null hypothesis.

## Results

***Kcnq1*$^{-/-}$ Neonatal Mice Exhibit a Long QT Phenotype.** To determine whether Kcnq1 plays a role in cardiac repolarization, we evaluated ECG recordings from anesthetized *Kcnq1*$^{+/+}$ and *Kcnq1*$^{-/-}$ neonates (Fig. 1). In general, similar ECG profiles were obtained for *Kcnq1*$^{+/+}$ and *Kcnq1*$^{-/-}$ neonates at baseline, although modest but significant increases in repolarization parameters (JT, QT, and

TABLE 1

ECG analysis of anesthetized neonatal *Kcnq1*$^{+/+}$ (WT) and *Kcnq1*$^{-/-}$ (KO) mice

ECG parameters were compared by two-sample Student's $t$ test, and $p$ values are tabulated. Data are mean ± S.E.M.

| Parameters | WT ($n = 28$) | KO ($n = 22$) | $p$ Value |
|---|---|---|---|
| RR (ms) | 131 ± 4 | 127 ± 3 | 0.49 |
| PR (ms) | 45 ± 1 | 46 ± 2 | 0.73 |
| P-wave amplitude (mV) | 0.34 ± 0.01 | 0.32 ± 0.02 | 0.38 |
| P-wave area (mV · ms · $10^{-1}$) | 15 ± 0.7 | 15 ± 0.9 | 0.92 |
| QRS duration (ms) | 6.8 ± 0.2 | 7.2 ± 0.2 | 0.18 |
| QRS amplitude (mV) | 1.5 ± 0.1 | 1.6 ± 0.1 | 0.27 |
| JT (ms) | 49 ± 2 | 57 ± 3 | 0.02 |
| QT (ms) | 55 ± 2 | 65 ± 3 | 0.008 |
| QTc (ms) | 49 ± 1 | 57 ± 2 | 0.003 |
| T-wave area (mV · ms · $10^{-1}$) | 62 ± 3 | 83 ± 7 | 0.008 |

TABLE 2

$\beta$-Adrenergic challenge exacerbates the long QT phenotype of *Kcnq1*$^{-/-}$ mice

ECG analysis of anesthetized neonatal *Kcnq1*$^{+/+}$ (WT) and *Kcnq1*$^{-/-}$ (KO) mice at baseline (BASE) and after intraperitoneal injection of isoproterenol (ISO) (0.17 mg/kg). The effect of isoproterenol was examined in each group of mice by paired Student's *t* test, and *p* values are tabulated.

| Parameters | WT ($n$ = 13) | | | KO ($n$ = 15) | | |
|---|---|---|---|---|---|---|
| | BASE | ISO | *p* Value | BASE | ISO | *p* Value |
| RR (ms) | 125 ± 7 | 116 ± 7 | 0.03 | 126 ± 4 | 117 ± 4 | 0.02 |
| PR (ms) | 44 ± 2 | 45 ± 3 | 0.90 | 47 ± 2 | 49 ± 3 | 0.55 |
| QRS duration (ms) | 7.1 ± 0.2 | 7.1 ± 0.3 | 0.50 | 7.3 ± 0.3 | 7.4 ± 0.2 | 0.82 |
| QT (ms) | 58 ± 2 | 57 ± 2 | 0.80 | 64 ± 3 | 72 ± 3 | 0.02 |
| QTc (ms) | 52 ± 1 | 53 ± 1 | 0.52 | 57 ± 1 | 66 ± 2 | 0.005 |
| T-wave area (mV · ms · $10^{-1}$) | 62 ± 3 | 74 ± 3 | 0.11 | 82 ± 3 | 151 ± 6 | 0.00002 |

QTc intervals and T-wave area) were found in the *Kcnq1*$^{-/-}$ group (Table 1). All other ECG parameters, including heart rate (RR interval), were not statistically different between these two groups of neonatal mice (Table 1).

**$\beta$-Adrenergic Stimulation Exacerbates Long QT Phenotype of *Kcnq1*$^{-/-}$ Neonatal Mice.** To determine whether $\beta$-adrenergic stimulation could differentially influence cardiac repolarization in *Kcnq1*$^{+/+}$ and *Kcnq1*$^{-/-}$ mice, we evaluated ECG parameters in a subset of neonates following injection of the $\beta$-adrenergic agonist, isoproterenol. The isoproterenol challenge resulted in a robust increase of all repolarization parameters (QT, QTc, and T-wave area) of *Kcnq1*$^{-/-}$ neonates but had no significant effect on repolarization parameters of *Kcnq1*$^{+/+}$ neonates (see Fig. 1 and Table 2). As a consequence, isoproterenol markedly exacerbated the relatively modest baseline differences in QT, QTc, and T-wave area ($p < 0.001$ for each) between *Kcnq1*$^{+/+}$ and *Kcnq1*$^{-/-}$ neonates. None of the other ECG parameters measured (RR, PR, and QRS values) were significantly different in *Kcnq1*$^{+/+}$ and *Kcnq1*$^{-/-}$ neonates in the presence of isoproterenol. No ventricular tachycardias were observed in either group. At the same time, the isoproterenol challenge was effective at stimulating cardiac $\beta$-adrenergic responses in both groups of mice, as reflected by the significant heart rate increases (shorter RR interval, Table 2). In contrast, control injections with saline in 14 *Kcnq1*$^{+/+}$ and seven *Kcnq1*$^{-/-}$ neonates had no significant effects on any of the ECG parameters of either group (data not shown). These results demonstrate that Kcnq1 is an important contributor to ventricular repolarization principally during $\beta$-adrenergic receptor stimulation in neonatal mice.

**$I_{Ks}$ Is Absent in *Kcnq1*$^{-/-}$ Myocytes.** To test the hypothesis that lack of $I_{Ks}$ may have contributed to the repolarization abnormalities of *Kcnq1*$^{-/-}$ mice, we attempted to record $I_{Ks}$ from voltage-clamped ventricular myocytes isolated from 3-day old *Kcnq1*$^{+/+}$ and *Kcnq1*$^{-/-}$ neonatal hearts. As also reported by other groups (Nuss and Marban, 1994; Wang et al., 1996; Drici et al., 1998), $I_{Ks}$ was present only in a fraction of the cells, and its density was small. $I_{Ks}$ was frequently superimposed on a relatively large nonspecific background current (Fig. 2A, left, top row). Thus, we used the following well-established biophysical and pharmacological criteria to ascertain the presence of $I_{Ks}$: 1) presence of time-dependent slowly activating outward current ($\tau_{Act}$ = 1.6 s, see Fig. 2B) upon membrane depolarization to +70 mV followed by slowly deactivating tail currents during repolarization to 0 mV (Fig. 2A, left, top row), 2) enhancement of both outward and tail currents in the presence of isoproterenol (Fig. 2A, middle, top row), and 3) sensitivity of both currents to the $I_{Ks}$-selective blocker, L-735,821 (1 $\mu$M, Fig. 2A, right). Using these criteria, clearly identifiable, L-735,821-sensitive $I_{Ks}$ (Fig. 2B) was present in 21 of 200 *Kcnq1*$^{+/+}$ myocytes tested. In contrast, none of the 103 *Kcnq1*$^{-/-}$ myocytes tested displayed any L-735,821-sensitive currents (Fig. 2A, bottom row) when examined similarly ($p <$

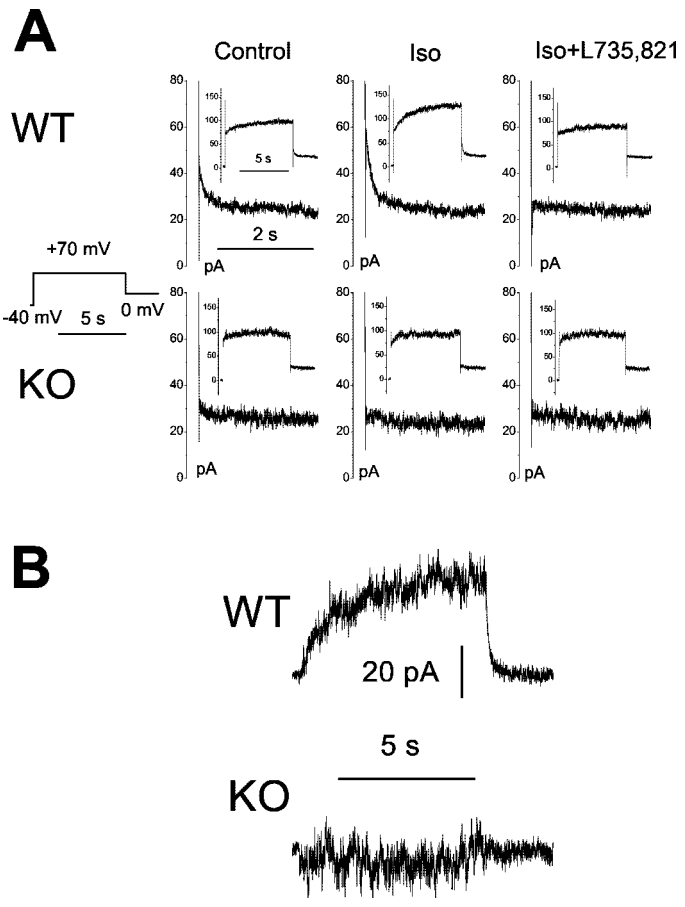


**Fig. 2.** Slowly activating delayed rectifier $K^+$ current ($I_{Ks}$) is absent in *Kcnq1*$^{-/-}$ (KO) cardiomyocytes. A, representative current traces (insets) and expanded view tail currents recorded from neonatal myocytes in control (no drug) condition (left), after isoproterenol (1 $\mu$M, middle), and in the presence of isoproterenol and the $I_{Ks}$-selective blocker, L-735,821 (1 $\mu$M, right). In four of 20 WT myocytes tested using this protocol, time-dependent outward currents with slowly deactivating tail currents resembling $I_{Ks}$ were up-regulated by isoproterenol and abolished by L-735,821. No isoproterenol-sensitive outward currents could be detected in nine *Kcnq1*$^{-/-}$ (KO) myocytes tested using the same protocol. B, digital subtraction of traces in middle and right panels yields the current component sensitive to L-735,821. No L-735,821-sensitive currents were found in KO myocytes.

0.001 by $\chi^2$ analysis). These results demonstrate that Kcnq1 is required for $I_{Ks}$ in neonatal mouse myocytes.

**Pharmacological Inhibition of $I_{Ks}$ Prolongs Ventricular Action Potential in Isolated Neonatal Mouse Heart.** To further confirm that lack of $I_{Ks}$ in cardiac tissue itself was responsible for the repolarization abnormalities, we recorded monophasic action potentials from ventricular epicardium in isolated perfused hearts harvested from 3-day-old neonates. To examine the effect of $I_{Ks}$ blockade, hearts were first perfused with solutions containing 200 nM isoproterenol to maximally stimulate $I_{Ks}$. The addition of isoproterenol shortened RR intervals (increased heart rate) and APDs in all groups (Fig. 3, B–D). On average, the $APD_{50}$ and $APD_{90}$ of *Kcnq1*$^{-/-}$ hearts were longer than those of heterozygous and wild-type mice, both at baseline and in the presence of isoproterenol (Fig. 3, C and D), but these differences were not found to be statistically significant in the small number of hearts evaluated here. However, in the presence of isoproterenol, pharmacological blockade of $I_{Ks}$ with L-735,821 significantly lengthened ventricular $APD_{90}$ in wild-type and heterozygous hearts but had no effect on ventricular APDs recorded from *Kcnq1*$^{-/-}$ hearts. The prolongation of APDs induced by L-735,821 in *Kcnq1*$^{+/+}$ hearts was reversible upon washout of the compound (Fig. 3, C and D). These results indicate that in the presence of isoproterenol, Kcnq1 and $I_{Ks}$ significantly contribute to cardiac repolarization in the neonatal mouse heart.

**Mapping the Major *Kcnq1* Transcript.** Generally, the mouse and human peptides are highly similar, as predicted by their respective cDNA sequences; however, the human KCNQ1 protein appeared to be longer at the N terminus by 64 amino acids (Yang et al., 1997). Examination of mouse genomic sequences indicated that the nucleotide sequences that would encode these 64 amino acids are immediately adjacent to those encoding the published mouse cDNA. To determine whether the mouse *Kcnq1* exon1$\alpha$ actually extended 5′ to include these sequences, we initiated RNase protection experiments using a series of overlapping antisense riboprobes targeted to this portion of the mouse *Kcnq1* gene (Fig. 4). With each probe, a single predominant band was protected (Fig. 4A). Collectively, the results from the three separate probes demonstrate that the 5′ boundary of this first exon extends beyond the published cDNA sequence to include an ATG start site in frame with the rest of the *Kcnq1* coding sequence (Fig. 4B). We have confirmed this result using an additional probe that overlaps this new start site and extends further in the 3′ direction to span exons 2 to 5 (Figs. 4, C and 4D). The predominant transcript is the 732-bp protected fragment in Fig. 4D, which accounted for 70 ± 9% ($n$ = 5) of the total Kcnq1 mRNA in the neonatal heart. Thus, the major *Kcnq1* mRNA species in both neonatal and adult mouse (data not shown) heart clearly extends further 5′ than previously thought and includes the newly identified upstream ATG (Fig. 4D). The new 5′ sequence of isoform 1 has been independently verified by RT-PCR experiments (data not shown) (GenBank accession no. AY331142). These results are summarized in Fig. 5, which shows the alignment of the full-length mouse and human peptide sequences for Kcnq1 isoform 1. These sequences share >88% overall amino acid identity and >91% amino acid conservation.

## Discussion

Our results demonstrate that *Kcnq1* expression is essential for native $I_{Ks}$ in ventricular myocytes, thereby confirming the conclusions from previous studies that used heterologous expression systems to show that co-expression of human *KCNQ1* and *KCNE1* genes yields $I_{Ks}$-like currents (Barhanin et al., 1996; Sanguinetti et al., 1996; Yang et al., 1997). In addition, Drici et al. (1998) showed that $I_{Ks}$ was absent from *Kcne1*-deficient neonatal mouse ventricular myocytes. Thus, both *Kcnq1* and *Kcne1* expression are required to produce native cardiac $I_{Ks}$.

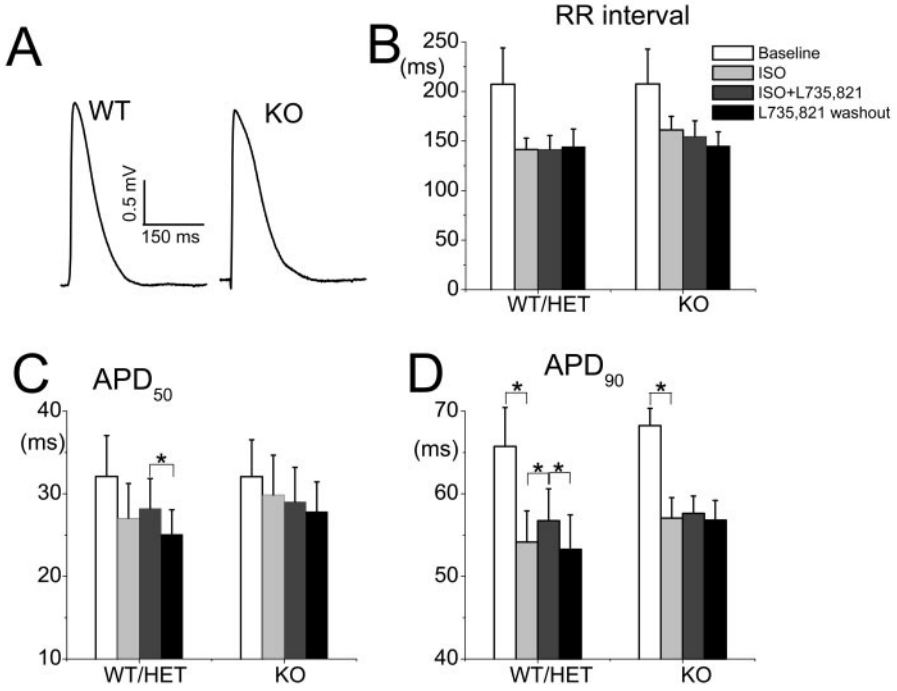


**Fig. 3.** Pharmacological inhibition of $I_{Ks}$ lengthens ventricular APD in isolated neonatal mouse heart. Ventricular monophasic action potentials were recorded from the epicardial surface of three *Kcnq1*$^{+/+}$ (WT), two *Kcnq1*$^{\pm}$ (HET), and four *Kcnq1*$^{-/-}$ (KO) isolated, Langendorff-perfused hearts harvested from 3-day-old neonates. A, representative monophasic action potentials recorded from WT and KO hearts. Data from WT and HET were pooled for analysis. Average RR interval (B), $APD_{50}$ (C), and $APD_{90}$ (D) are compared at baseline, in the presence of isoproterenol (200 nM), in presence of isoproterenol and L-735,821 (1 $\mu$M), and after washout of L-735,821 (isoproterenol still present in the perfusate). L-735,821 significantly prolonged the $APD_{50}$ and $APD_{90}$ in WT/HET hearts but had no effect in KO hearts. Data are mean ± S.E.M. *, $p < 0.05$ by paired Student's $t$ test. Experiments were performed at 36.5°C.

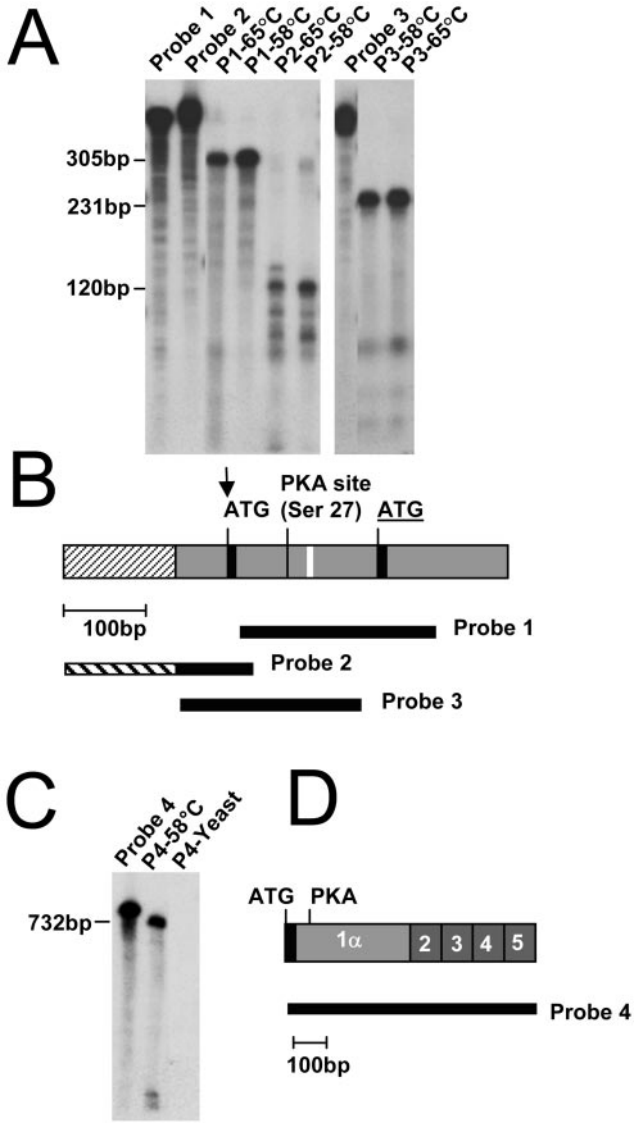


**Fig. 4.** Redefining exon1$\alpha$. A, RNase protection assays define the exon1$\alpha$ structure. Undigested probes are shown in lanes 1, 2, and 7 (for probes 1, 2, and 3, respectively). Each probe was hybridized with RNA isolated from neonatal mouse heart at 58° and 65°C, as indicated. The size of the predominant protected band for each probe used is indicated to the left of the autoradiograms. No protected products were observed when the probes were hybridized to yeast RNA in the same experiment (data not shown). B, schematic drawing of the proposed 5′ structure of mouse *Kcnq1*. The cartoon shows exon1$\alpha$ (gray bar) and the contiguous upstream genomic DNA (hatched bar). The regions of Kcnq1 transcript "protected" from RNase digestion for each of the three overlapping probes used in the experiment are indicated in black beneath the structure diagram. Note that the 5′ region of probe 2 was not protected (hatched line). These results indicate that the 5′ boundary of exon1$\alpha$ is approximately 190 bp upstream of the previously published (Paulsen et al., 1998) boundary (white line). Thus, exon1$\alpha$ now contains two prospective ATG start sites (black bands) where the more 5′ ATG (highlighted by arrow) is in a strong translational context (Kozak, 1999) and is in-frame with a consensus PKA-phosphorylation site (Ser27) that has been shown to be important for regulation of human KCNQ1 (Marx et al., 2002). The second ATG (underlined) represents the site previously thought to be the translational start site of mouse Kcnq1. C, the predominant *Kcnq1* RNA includes full exon1$\alpha$. Labeled probe 4 (left lane) was hybridized with mouse neonatal heart RNA at 58°C and subjected to RNase protection assays. A fully protected fragment (732 bp) was detected with probe 4 (middle lane). No protected products were observed when the probe was hybridized to yeast RNA in the same experiment (right lane). D, cartoon of the 5′ structure of the major *Kcnq1* transcript (top line) and the corresponding region protected by probe 4 (bottom black line).

Our results suggest that $I_{Ks}$ contributes to cardiac repolarization of neonatal mice because pups lacking $I_{Ks}$ and Kcnq1 have significantly longer "baseline" JT, QT, and QTc intervals than their wild-type siblings (Table 1). The fact that isoproterenol significantly exacerbates the differences in these repolarization parameters between $Kcnq1^{-/-}$ and $Kcnq1^{+/+}$ neonates is consistent with the well-established observation that $I_{Ks}$ is dramatically enhanced by activation of $\beta$-adrenergic signal transduction pathways (Walsh and Kass, 1988; An et al., 1999; Marx et al., 2002). Our results are also consistent with previous studies showing that pharmacological block of $I_{Ks}$ in canine ventricular "wedge" and myocyte preparations primarily affected repolarization during $\beta$-adrenergic stimulation (Shimizu and Antzelevitch, 1998; Han et al., 2001).

Enhanced $I_{Ks}$ is likely to counter the well-established stimulatory effects of PKA on L-type $Ca^{2+}$ channels or $Ca^{2+}$ release channels, which would prolong cardiac action potentials. Deletion of KCNQ1 (or pharmacological block of $I_{Ks}$) might lead to an imbalanced response to adrenergic receptor stimulation, with the net effect of action potential prolongation, as demonstrated in Fig. 3. Interestingly, neonatal mouse action potential wave shape closely resembled action potentials recorded from dogs and humans (Franz et al., 1987), which is certainly not the case in adult mice (Knollmann et al., 2001). These findings further strengthen the utility of the neonatal mouse heart as a model for studying the electrophysiological and pharmacological consequences of Kcnq1 mutations.

Notably, the effect of KCNQ1 deletion or pharmacological block of $I_{Ks}$ on action potential durations measured in isolated hearts was much more modest than that on the QT interval in vivo (3–4 ms versus 6–8 ms, respectively; compare Fig. 3 and Table 2). A likely explanation for this apparent discrepancy is that action potentials were recorded only from discrete regions of the epicardial surface of the heart. Thus, action potentials of deeper tissue layers may have been affected to greater extents and could be responsible for the prominent T-wave changes and QT prolongation observed in vivo (Table 2). This point is not without merit since both Kcnq1 and Kcne1 have been shown to be expressed throughout both ventricles at comparable stages of development (Franco et al., 2001). Thus, the ECG data (JT, QT, and QTc) likely represent a more accurate general measure of cardiac repolarization, whereas the MAP data provides more specific information about repolarization at localized sites on the ventricular surface of the heart. Even so, it is clear that the ECG and MAP data tend to corroborate each other in this case, thereby supporting the notion that Kcnq1 and $I_{Ks}$ significantly contribute to cardiac repolarization in the neonatal mouse heart, especially when $\beta$-adrenergic receptors are activated.

In contrast to our results from $Kcnq1^{-/-}$ neonates, $Kcne1^{-/-}$ neonates had no apparent QT prolongation relative to wild-type controls (Kupershmidt et al., 1999), despite the absence of $I_{Ks}$ in both strains of genetically disrupted mice. Notably, the QT interval measurements of $Kcne1^{-/-}$ neonates in the aforementioned study were significantly longer and more variable than those reported here (Table 1) and elsewhere (Wang et al., 2000). Thus, the modest differences in repolarization that we observed during baseline ECG recordings of $Kcnq1^{-/-}$ versus $Kcnq1^{+/+}$ neonates may

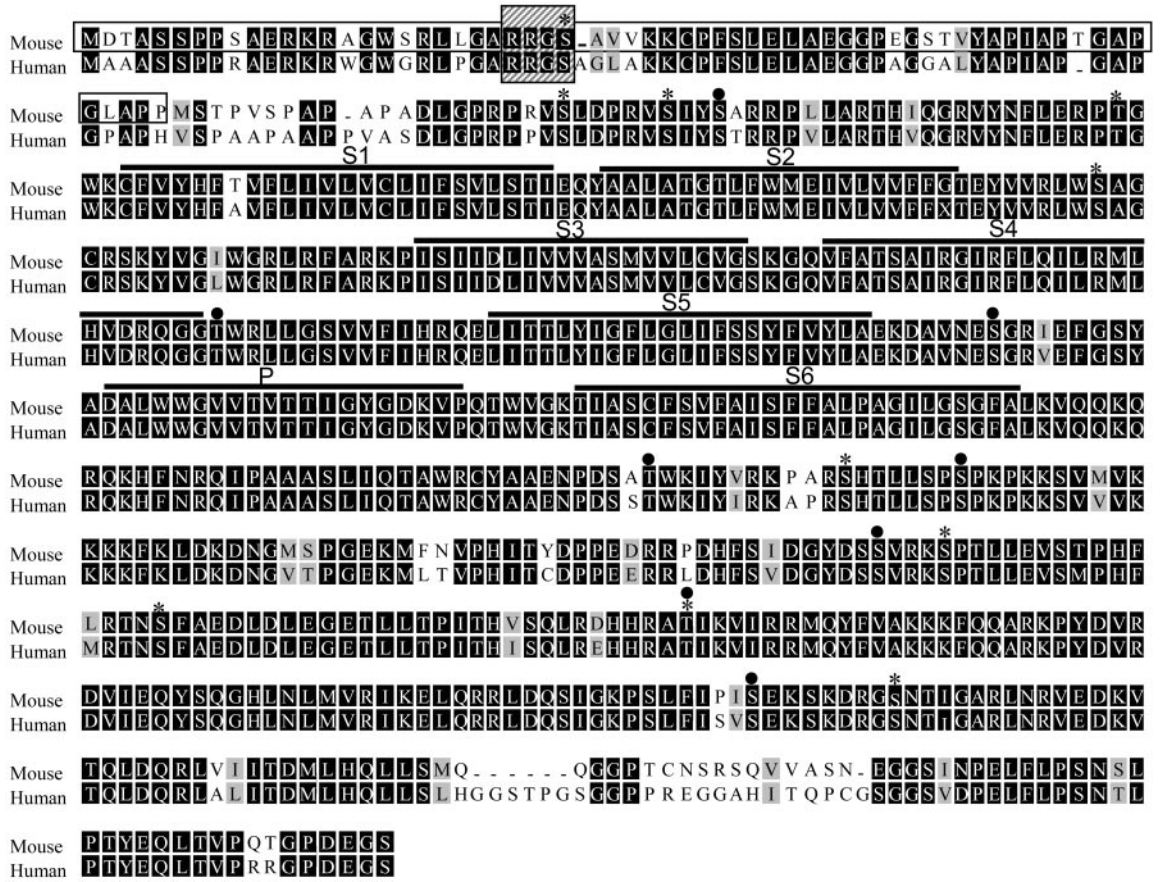


**Fig. 5.** Comparison of amino acid sequence from mouse and human Kcnq1. Alignment and formatting were performed using GCG-Clustal W and GCG-Box Shade Utilities, respectively. The additional 64 amino acids of N-terminal sequence of mouse *Kcnq1* are boxed. The position of the consensus PKA phosphorylation site (Ser27) conserved between mouse and human is indicated with a gray hatched box. Identical residues are shaded in black, and homologous residues are shaded in gray. The secondary structure is given according to Barhanin et al. (1996), and it shows the six putative transmembrane domains S1 to S6 and the pore region (P domain) (black lines). The prospective PKC (●) and PKA (∗) phosphorylation sites indicated were predicted using the PhosphoBase v2.0 prediction program (Kreegipuu et al., 1999). The sequence of human KCNQ1 was taken from Neyroud et al. (1999), and the sequence of mouse Kcnq1 is derived from this work (GenBank accession no. AY331142).

not have been apparent in the Kcne1 study. Alternatively, since Kcnq1 is capable of forming functional homomeric channels (Barhanin et al., 1996) or may associate with other Kcne-like subunits (Abbott and Goldstein, 2002), the absence of such currents could, in theory, also contribute to the long QT phenotype of *Kcnq1*$^{-/-}$ neonates; however, the slow activation kinetics of the L-735,821-sensitive currents recorded in the present study ($\tau_{Act}$ = 1.6s) are consistent with those previously reported for $I_{Ks}$ (Salata et al., 1996; Seebohm et al., 2001) and, therefore, do not support the presence of non-$I_{Ks}$ Kcnq1-dependent currents in neonatal mouse ventricular myocytes. Nevertheless, we cannot unequivocally rule out this possibility. Future experiments that directly compare *Kcne1*$^{-/-}$ and *Kcnq1*$^{-/-}$ neonates should help to resolve this issue.

Remarkably, the mouse and human Kcnq1 peptide sequences are highly conserved, with >88% overall amino acid identity and >91% amino acid conservation for isoform 1, the predominant cardiac transcript found in both species (Yang et al., 1997; present study). All of the putative PKA and PKC phosphorylation sites are conserved, including Ser27, which was shown recently to be an important target for PKA-mediated phosphorylation of human KCNQ1 (Marx et al., 2002). Interestingly, another recent study has identified a novel S140G "gain-of-function" mutation in human *KCNQ1* that is linked to a hereditary persistent form of atrial fibrillation (Chen et al., 2003). The Ser140 residue, found in the S1 transmembrane segment of KCNQ1, is also conserved in mouse Kcnq1, indicating that the mouse model may prove useful for probing the underlying molecular genetics of atrial and ventricular arrhythmias. In addition, the size of the mouse Kcnq1 protein (668 amino acids) is similar to the human KCNQ1 protein (676 amino acids), and the major isoform expressed in both human (Yang et al., 1997) and mouse hearts is isoform 1. Thus, the mouse *Kcnq1* gene appears to be highly conserved with the human *KCNQ1* gene in both form and function.

### References

Abbott GW and Goldstein SA (2002) Disease-associated mutations in KCNE potassium channel subunits (MiRPs) reveal promiscuous disruption of multiple currents and conservation of mechanism. *FASEB J* **16:**390–400.

Ackerman MJ, Tester DJ, and Porter CJ (1999) Swimming, a gene-specific arrhythmogenic trigger for inherited long QT syndrome. *Mayo Clin Proc* **74:**1088–1094.

Ali RH, Zareba W, Moss AJ, Schwartz PJ, Benhorin J, Vincent GM, Locati EH, Priori S, Napolitano C, Towbin JA, et al. (2000) Clinical and genetic variables associated with acute arousal and nonarousal-related cardiac events among subjects with long QT syndrome. *Am J Cardiol* **85:**457–461.

An R, Heath BM, Higgins JP, Koch WJ, Lefkowitz RJ, and Kass RS (1999) Beta2-adrenergic receptor overexpression in the developing mouse heart: evidence for targeted modulation of ion channels. *J Physiol* **516:**19–30.

An RH, Davies MP, Doevendans PA, Kubalak SW, Bangalore R, Chien KR, and Kass RS (1996) Developmental changes in beta-adrenergic modulation of L-type $Ca^{2+}$ channels in embryonic mouse heart. *Circ Res* **78:**371–378.

Barhanin J, Lesage F, Guillemare E, Fink M, Lazdunski M, and Romey G (1996)

KvLQT1 and IsK (minK) proteins associate to form the IKs cardiac potassium current. *Nature (Lond)* **384:**78–80.
Casimiro M, Knollmann BK, Ebert SN, Vary J, Grinberg A, and Pfeifer K (2001) Targeted disruption of the Kvlqt1 gene produces a mouse model of Jervell and Lange-Nielsen Syndrome. *Proc Natl Acac Sci USA* **98:**2526–2531.
Chen YH, Xu SJ, Bendahhou S, Wang XL, Wang Y, Xu WY, Jin HW, Sun H, Su XY, Zhuang QN, et al. (2003) KCNQ1 gain-of-function mutation in familial atrial fibrillation. *Science (Wash DC)* **299:**251–254.
Drici MD, Arrighi I, Chouabe C, Mann JR, Lazdunski M, Romey G, and Barhanin J (1998) Involvement of IsK-associated $K^+$ channel in heart rate control of repolarization in a murine engineered model of Jervell and Lange-Nielsen syndrome. *Circ Res* **83:**95–102.
Franco D, Demolombe S, Kupershmidt S, Dumaine R, Dominguez JN, Roden D, Antzelevitch C, Escande D, and Moorman AF (2001) Divergent expression of delayed rectifier K(+) channel subunits during mouse heart development. *Cardiovasc Res* **52:**65–75.
Franz MR, Bargheer K, Rafflenbeul W, Haverich A, and Lichtlen PR (1987) Monophasic action potential mapping in human subjects with normal electrocardiograms: direct evidence for the genesis of the T wave. *Circulation* **75:**379–386.
Gould T and Pfeifer K (1998) Imprinting of mouse Kvlqt1 is developmentally regulated. *Hum Mol Genet* **7:**483–487.
Hamill OP, Marty A, Neher E, Sakmann B, and Sigworth FJ (1981) Improved patch-clamp techniques for high-resolution current recording from cells and cell-free membrane patches. *Pflugers Arch* **391:**85–100.
Han W, Wang Z, and Nattel S (2001) Slow delayed rectifier current and repolarization in canine cardiac Purkinje cells. *Am J Physiol Heart Circ Physiol* **280:**H1075–H1080.
Knollmann BC, Katchman AN, and Franz MR (2001) Monophasic action potential recordings from intact mouse heart: validation, regional heterogeneity and relation to refractoriness. *J Cardiovasc Electrophysiol* **12:**1286–1294.
Kozak M (1999) Initiation of translation in prokaryotes and eukaryotes. *Gene* **234:** 187–208.
Kreegipuu A, Blom N, and Brunak S (1999) PhosphoBase, a database of phosphorylation sites: release 2.0. *Nucleic Acids Res* **27:**237–239.
Kupershmidt S, Yang T, Anderson ME, Wessels A, Niswender KD, Magnuson MA, and Roden DM (1999) Replacement by homologous recombination of the minK gene with lacZ reveals restriction of minK expression to the mouse cardiac conduction system. *Circ Res* **84:**146–152.
Lee MP, Ravenel JD, Hu RJ, Lustig LR, Tomaselli G, Berger RD, Brandenburg SA, Litzi TJ, Bunton TE, Limb C, et al. (2000) Targeted disruption of the Kvlqt1 gene causes deafness and gastric hyperplasia in mice. *J Clin Invest* **106:**1447–1455.
Lengyel C, Iost N, Virag L, Varro A, Lathrop DA, and Papp JG (2001) Pharmacological block of the slow component of the outward delayed rectifier current (I(Ks)) fails to lengthen rabbit ventricular muscle QT(c) and action potential duration. *Br J Pharmacol* **132:**101–110.
Li RA, Miake J, Hoppe UC, Johns DC, Marban E, and Nuss HB (2001) Functional consequences of the arrhythmogenic G306R KvLQT1 $K^+$ channel mutant probed by viral gene transfer in cardiomyocytes. *J Physiol* **533:**127–133.
Lynch JJ Jr, Salata JJ, Wallace AA, Stump GL, Gilberto DB, Jahansouz H, Liverton NJ, Selnick HG, and Claremon DA (2002) Antiarrhythmic efficacy of combined I(Ks) and beta-adrenergic receptor blockade. *J Pharmacol Exp Ther* **302:**283–289.
Marx SO, Kurokawa J, Reiken S, Motoike H, D'Armiento J, Marks AR, and Kass RS (2002) Requirement of a macromolecular signaling complex for beta adrenergic receptor modulation of the KCNQ1-KCNE1 potassium channel. *Science (Wash DC)* **295:**496–499.
Mitchell GF, Jeron A, and Koren G (1998) Measurement of heart rate and Q-T interval in the conscious mouse. *Am J Physiol* **274:**H747–H751.
Neyroud N, Richard P, Vignier N, Donger C, Denjoy I, Shkolnikova M, Pesce R, Chevalier P, Hainque B, Schwartz K, et al. (1999) Genomic organization of the KCNQ1 $K^+$ channel gene and identification of C-terminal mutations in the long-QT syndrome. *Circ Res* **84:**290–297.
Nuss HB and Marban E (1994) Electrophysiological properties of neonatal mouse cardiac myocytes in primary culture. *J Physiol* **479:**265–279.
Paulsen M, Davies KR, Bowden LM, Villar AJ, Franck O, Fuermann M, Dean WL, Moore TF, Rodrigues N, Davies KE, et al. (1998) Syntenic organization of the mouse distal chromosome 7 imprinting cluster and the Beckwith-Wiedemann syndrome region in chromosome 11p15.5. *Hum Mol Genet* **7:**1149–1159.
Roden DM and Spooner PM (1999) Inherited long QT syndromes: a paradigm for understanding arrhythmogenesis. *J Cardiovasc Electrophysiol* **10:**1664–1683.
Salata JJ, Jurkiewicz NK, Jow B, Folander K, Guinosso PJ Jr, Raynor B, Swanson R, and Fermini B (1996) IK of rabbit ventricle is composed of two currents: evidence for IKs. *Am J Physiol* **271:**H2477–H2489.
Sanguinetti M, Curran M, Zou A, Shen J, Spector P, Atkinson D, and Keating M (1996) Coassembly of KvLQT1 and minK (IsK) proteins to form cardiac IKs potassium channel. *Nature (Lond)* **384:**80–83.
Sanguinetti MC and Jurkiewicz NK (1990) Two components of cardiac delayed rectifier $K^+$ current: differential sensitivity to block by class III antiarrhythmic agents. *J Gen Physiol* **96:**195–215.
Schwartz PJ, Priori SG, Spazzolini C, Moss AJ, Vincent GM, Napolitano C, Denjoy I, Guicheney P, Breithardt G, Keating MT, et al. (2001) Genotype-phenotype correlation in the long-QT syndrome: gene-specific triggers for life-threatening arrhythmias. *Circulation* **103:**89–95.
Seebohm G, Lerche C, Busch AE, and Bachmann A (2001) Dependence of I(Ks) biophysical properties on the expression system. *Pflugers Arch* **442:**891–895.
Selnick HG, Liverton NJ, Baldwin JJ, Butcher JW, Claremon DA, Elliott JM, Freidinger RM, King SA, Libby BE, McIntyre CJ, et al. (1997) Class III antiarrhythmic activity in vivo by selective blockade of the slowly activating cardiac delayed rectifier potassium current IKs by (R)-2-(2,4-trifluoromethyl)-N-[2-oxo-5-phenyl-1-(2,2,2-trifluoroethyl)- 2,3-dihydro-1H-benzo[e][1,4]diazepin-3-yl]acetamide. *J Med Chem* **40:**3865–3868.
Shimizu W and Antzelevitch C (1998) Cellular basis for the ECG features of the LQT1 form of the Long-QT Syndrome: effects of $\beta$-adrenergic agonists and antagonists and sodium channel blockers on transmural dispersion of repolarization and torsades de pointes. *Circulation* **98:**2314–2322.
Song GL, Tang M, Liu CJ, Luo HY, Liang HM, Hu XW, Xi JY, Gao LL, Fleischmann B, and Hescheler J (2002) Developmental changes in functional expression and beta-adrenergic regulation of I(f) in the heart of mouse embryo. *Cell Res* **12:**385–394.
Tosaka T, Casimiro MC, Rong Q, Tella S, Oh M, Katchman AN, Pezzullo JC, Pfeifer K, and Ebert SN (2003) Nicotine induces a long QT phenotype in Kcnq1-deficient mouse hearts. *J Pharmacol Exp Ther* **306:**980–987.
Walsh KB and Kass RS (1988) Regulation of a heart potassium channel by protein kinase A and C. *Science (Wash DC)* **242:**67–69.
Wang L, Feng ZP, Kondo CS, Sheldon RS, and Duff HJ (1996) Developmental changes in the delayed rectifier $K^+$ channels in mouse heart. *Circ Res* **79:**79–85.
Wang L, Swirp S, and Duff H (2000) Age-dependent response of the electrocardiogram to K(+) channel blockers in mice. *Am J Physiol Cell Physiol* **278:**C73–C80.
Yang WP, Levesque PC, Little WA, Conder ML, Shalaby FY, and Blanar MA (1997) KvLQT1, a voltage-gated potassium channel responsible for human cardiac arrhythmias. *Proc Natl Acad Sci USA* **94:**4017–4021.

**Address correspondence to:** Dr. Steven N. Ebert, Department of Pharmacology, Georgetown University Medical Center, 3900 Reservoir Road, NW, Washington, DC 20007. E-mail:eberts@georgetown.edu